World Academy of Science, Engineering and Technology
International Journal of Biomedical and Biological Engineering
Vol:10, No:3, 2016

Distinction between Manifestations of Diabetic Retinopathy and Dust Artifacts Using Three-Dimensional HSV Color Space

Naoto Suzuki

Abstract**—**Many ophthalmologists find it difficult to distinguish between small retinal hemorrhages and dust artifacts when using fundus photography for the diagnosis of diabetic retinopathy. Six patients with diabetic retinopathy underwent fundus photography, which revealed dust artifacts in the photographs of some patients. We constructed an experimental device similar to the optical system of the fundus camera and colored the fundi of the artificial eyes with khaki, sunset, rose and sunflower colors. Using the experimental device, we photographed dust artifacts using each artificial eyes. We used Scilab 5.4.0 and SIVP 0.5.3 softwares to convert the red, green, and blue (RGB) color space to the hue, saturation, and value (HSV) color space. We calculated the differences between the areas of manifestations and perimanifestations and the areas of dust artifacts and periartifacts using average HSVs. The V values in HSV for the manifestations were as follows: hemorrhages, 0.06 ± 0.03; hard exudates, −0.12 ± 0.06; and photocoagulation marks, 0.07 ± 0.02. For dust artifacts, visualized in the human and artificial eyes, the V values were as follows: human eye, 0.19 ± 0.03; khaki, 0.41 ± 0.02; sunset, 0.43 ± 0.04; rose, 0.47 ± 0.11; and sunflower, 0.59 ± 0.07. For the human and artificial eyes, we calculated two sensitivity values of dust artifacts compared to manifestation areas. V values of the HSV color space enabled the differentiation of small hemorrhages, hard exudates, and photocoagulation marks from dust artifacts.

Keywords**—**Diabetic retinopathy, HSV color space, small hemorrhages, hard exudates, photocoagulation marks

I. Introduction

DIABETIC complications manifest in the liver, nerves, and eyes, leaving approximately 40% of the patients with retinopathy. At a high rate of 19% of acquired blindness, diabetic retinopathy is the major cause of acquired blindness. Approximately 3000 people lose their eyesight every year because of this disease [1]. Studies have shown that the number of diabetics in America has likely increased from 16 million to 30 million since 1999 [2], whereas the number of diabetics in Japan, including potential patients, was only 16.2 million in 2005 [1]. Unfortunately, diabetic retinopathy is a progressive disease, which modern medicine is unable to completely cure. Consequently, early diagnosis through a careful ophthalmic examination is critical in preventing acquired blindness [3]-[5]. However, many retinal hemorrhages are too small to be visible [6]-[7]. This is particularly true when patients have cloudy ocular media, like a cataract. As shown in Fig. 1, the hemorrhage outlines are blurred in Fig. 1 (b), and as shown in the enlarged image of the small hemorrhage obtained by Fig. 1 (a), the hemorrhage color is faded. Although it is important for ophthalmologists to distinguish between small hemorrhages and dust artifacts on fundus photographs, hard exudates or photocoagulation marks can look similar to these artifacts. This makes the accurate diagnosis more difficult.

N. Suzuki is with National Institute of Technology, Numazu College, Numazu, Shizuoka, 4108501, Japan (phone: 81-55-926-5789; fax: 81-55-926-5780; e-mail: n-suzuki@numazu-ct.ac.jp).

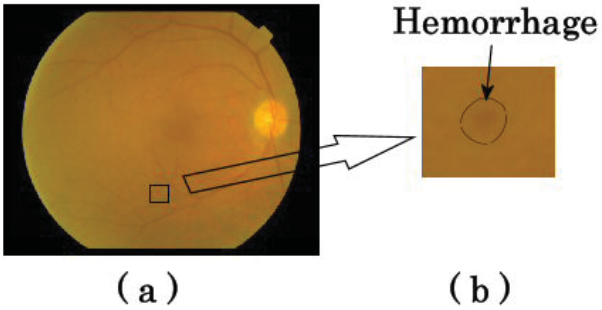

Fig. 1 The area of small retinal hemorrhages in the fundus photograph of a patient with diabetic retinopathy

When we consider what causes image artifacts, we found, for example, that white spots may appear in photographs taken using a strobe light in a room where dust particles are present [8]-[9]. Dust particles on the object lens may further cause black spots to appear in photographs. These white or black spots are called dust artifacts [10]-[12]. A fundus camera consists of a color camera, a strobe light, an object lens, several different lenses, a mirror, a mirror with a hole, and aperture stops [13]-[14]. If dust particles adhere to any of these optical components, they may be visible on the fundus photograph. For the purpose of this study, we understood that we could divide some artifact research studies performed on this subject into two research areas. The first research area determines how to remove dust artifacts from photographs. The second research area shows how to remove dust particles from some equipment [15]-[19]. However, these studies were not related to the medical diagnosis that involves the use of a fundus camera. In these studies, the researchers were unable to completely delete the image artifacts from photographs and did not address the issue of dust artifacts. To address this gap, we used a strobe light to photograph dust particles in a room. We also photographed dust particles present on a lens. We then attempted to distinguish between small retinal hemorrhages and dust artifacts using a hue, lightness, and saturation color space [20]. Because of many components in the fundus photographs,

such as blood vessels, optic discs, and optic nerves, it is very difficult to distinguish these complicated forms using image processing. To detect early diabetic retinopathy, we conducted a verification experiment that distinguishes small hemorrhages, hard exudates, and photocoagulation marks from dust artifacts. We then processed photographs using a hue, saturation, and value (HSV) color space and evaluated the sensitivity that could distinguish between manifestation areas and dust artifacts.

II. Experiment Method

A. Fundus Photography

We photographed the eyes of five patients with diabetic retinopathy and used two areas of hemorrhages from each patient.

B. Experimental Device

Because it is difficult for ophthalmologists to identify dust artifacts in fundus photographs of the human eye, we constructed both an experimental device and an artificial eye. The experimental device uses the same optical systems as a fundus camera (Fig. 2): an illumination optical system and a photographic optical system. In the illumination optical system, light from a strobe light passes through the aperture stops to reach the artificial eye, whereas in the photographic optical system, light reflected from the fundus of the artificial eye passes through a mirror with a hole to reach the color camera.

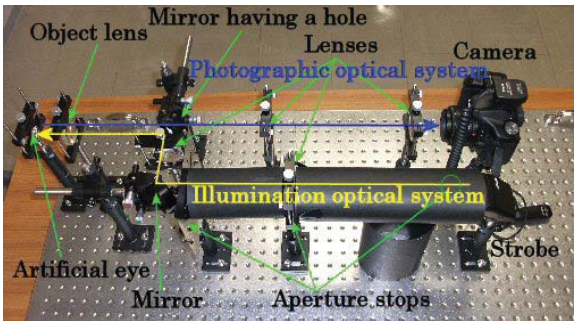

Fig. 2 Experimental device

C. Artificial Eye

The artificial eye referred to is the Gullstrand artificial eye [21], which consists of a plano-convex lens, black spacer, and hemispherical cup, as shown in Fig. 3. The plano-convex lens (made in Edmund Optics Japan Co. Ltd.) was 20 mm in diameter, 17.4 mm in back focal length, and 4.6 mm in thickness. The black spacer was 20 mm in outer diameter and 1 mm in thickness. The hemispherical cup was 20 mm in outer diameter and 0.5 mm in thickness. The distance from the surface of the plano-convex lens to the fundus of the artificial eye was 22 mm. The hemispherical cup was made from polyethylene terephthalate and was painted using four matt color sprays (Asahipen Corp., Osaka, Japan): light khaki, sunset, rose red, and sunflower.

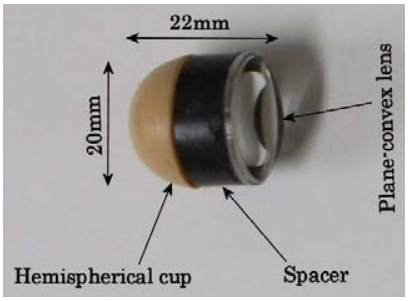

Fig. 3 Artificial eye

D. Dust Artifact

Dust artifacts with the artificial eye of each of the colored fundi were photographed five times with the experimental device, as shown in Fig. 4. House dust fragments, all less than 2 mm, were placed on the object lens on a narrow line, 0.128 mm in diameter, made from fluorocarbon.

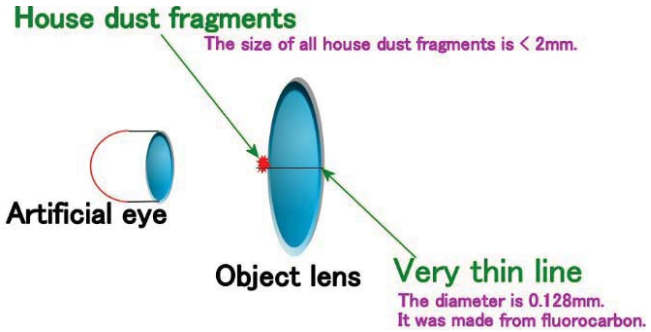

Fig. 4 House dust fragments were placed on the object lens while photographing dust artifacts

E. Analysis

All images were analyzed using the numerical computing languages Scilab 5.4.0 and SIVP 0.5.3 (Scilab image processing toolbox), which changed the red, green, and blue (RGB) color space into the hue, saturation, and value (HSV) color space. The software interpreted each HSV color space value as a three-dimensional graph, which was subsequently modified using a Gaussian filter. Filter size was determined by hsize parameter, which is defined as the size of a square matrix. On analysis, hsize was determined to be 13 and the sigma parameter to be 0.5.

III. Results

A. Calculating the Difference between Two Areas Using Average HSVs

We calculated the difference between the manifestation and perimanifestation areas and between the dust artifact and periartifact areas using average HSVs.

B. V Values for Hemorrhages, Hard Exudates, and Photocoagulation Marks

We extracted diabetic retinopathy manifestation areas from the fundus images. Fig. 5 shows the three-dimensional graph of V values for hemorrhages; the upper area indicates perihemorrhages, and the lower area indicates hemorrhages.

The difference between hemorrhages and perihemorrhages was 0.06 ± 0.03. Fig. 6 shows the V values for the hard exudates; the upper area indicates hard exudates, and the lower area indicates periexudates. The difference between hard exudates and periexudates was −0.12 ± 0.06. Fig. 7 shows the V values for the photocoagulation marks; the upper area indicates periphotocoagulation marks, and the lower area indicates photocoagulation marks. The difference between the photocoagulation and periphotocoagulation marks was 0.07 ± 0.02.

C. V Values for Dust Artifacts Visualized in the Human and Artificial Eyes

We used dust artifacts that appeared in the fundus image of the human eye as well as dust artifacts photographed with the four artificial eyes, each having a colored fundus. We then conducted a three-dimensional analysis of all dust artifacts. Fig. 8 shows the V values for dust artifacts visualized in the human eye. Here the upper area indicates periartifacts, and the lower area indicates dust artifacts. The difference between dust artifacts and periartifacts was 0.19 ± 0.03. Fig. 9 (sunflower), 10 (rose), 11 (sunset), and 12 (khaki) show the V values for dust artifacts visualized in the artificial eye of each colored fundus. Here the upper area indicates periartifacts, and the lower area indicates dust artifacts. The differences between dust artifacts and periartifacts were as follows: khaki, 0.41 ± 0.02; sunset, 0.43 ± 0.04; rose, 0.47 ± 0.11; and sunflower, 0.59 ± 0.07.

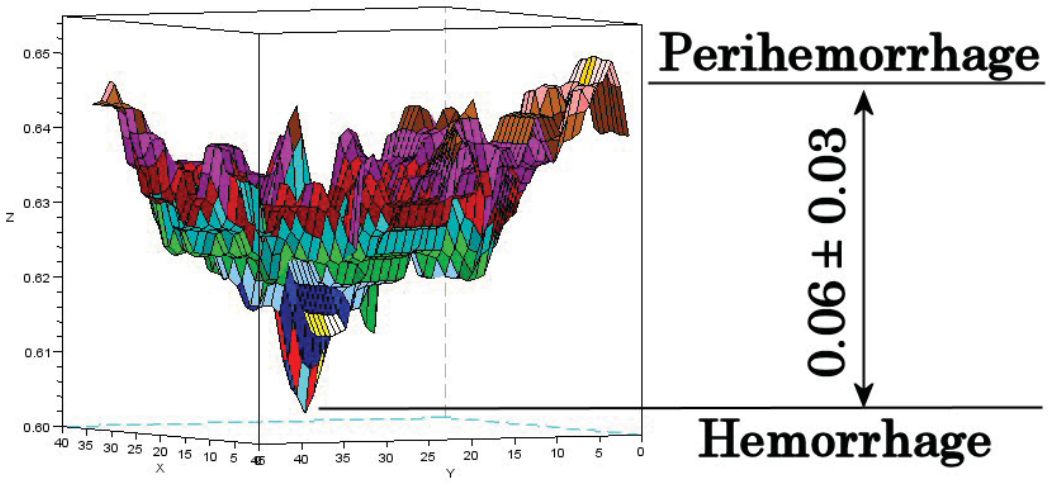

Fig. 5 V values for hemorrhages

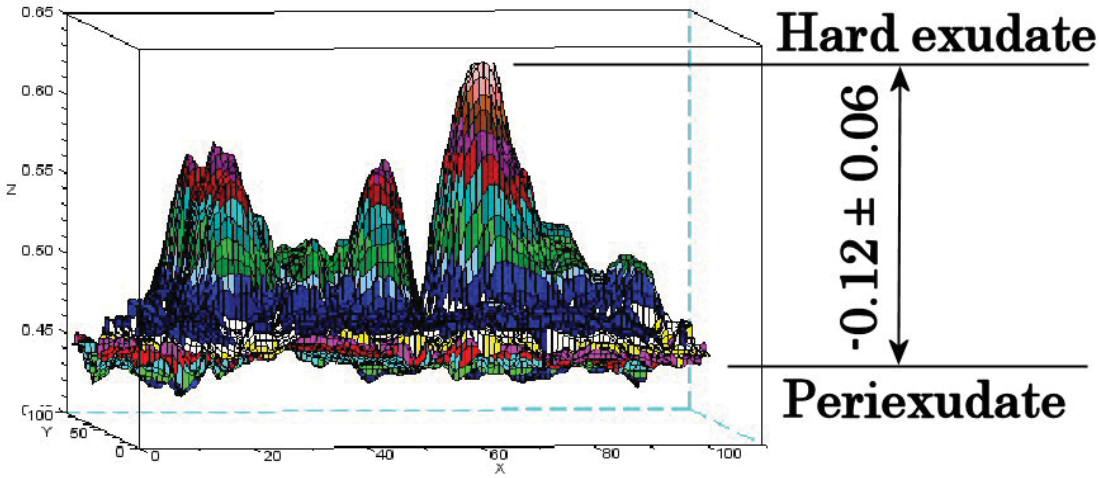

Fig. 6 V values for hard exudates

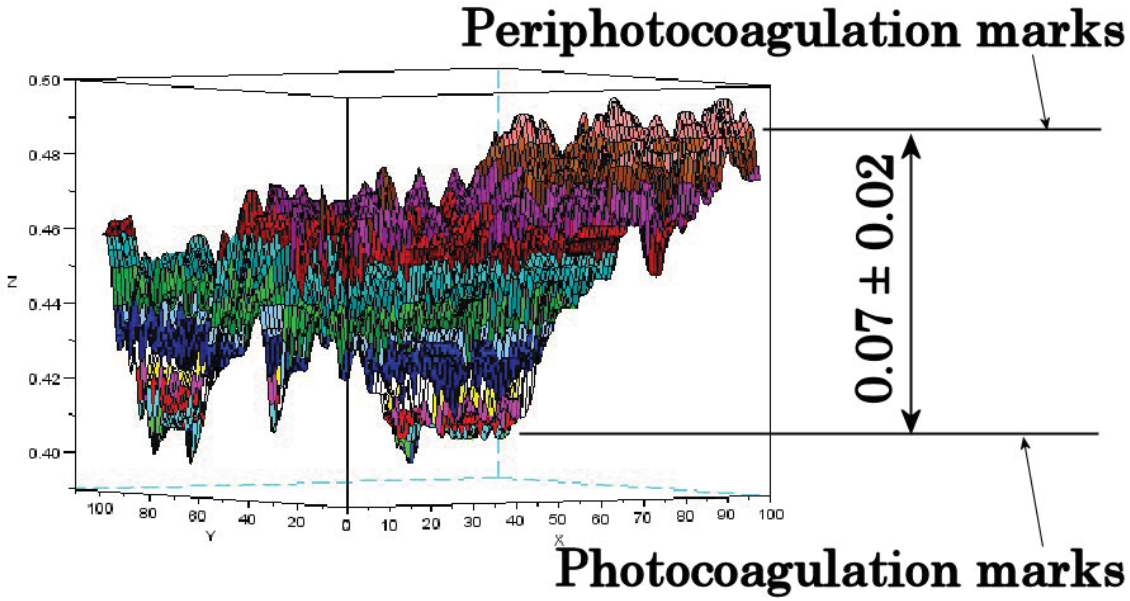

Fig. 7 V values for photocoagulation marks

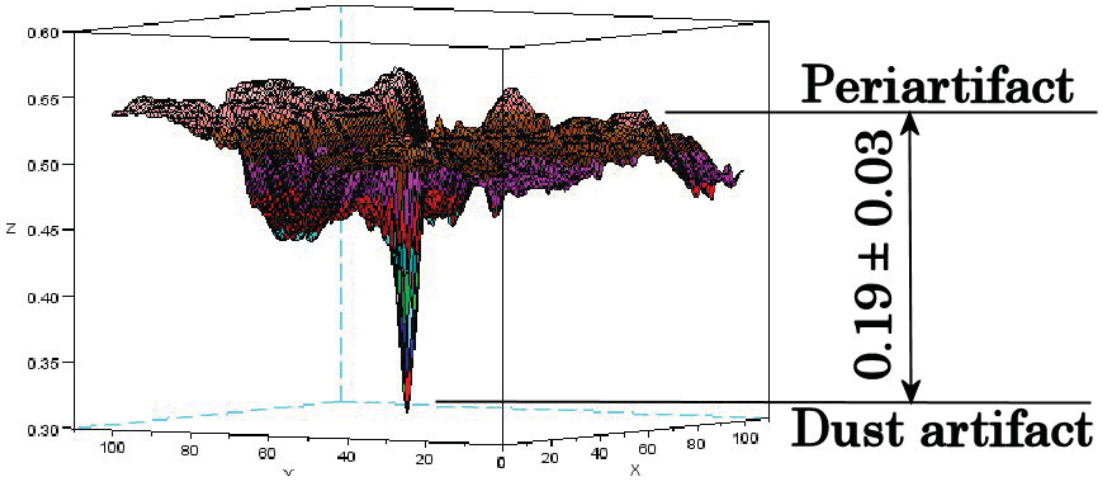

Fig. 8 V values for dust artifacts visualized in the human eye

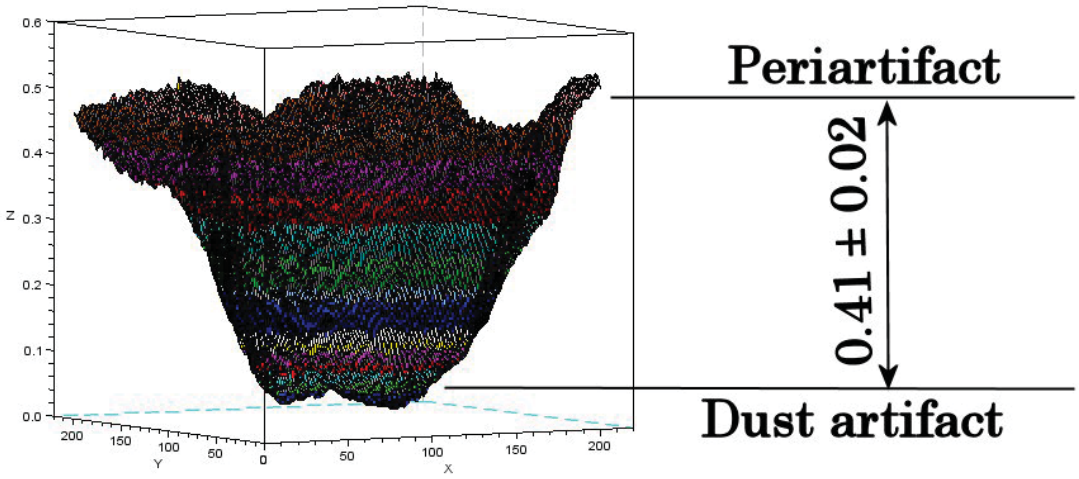

Fig. 9 V value for dust artifacts visualized in the artificial eye with a khaki-colored fundus

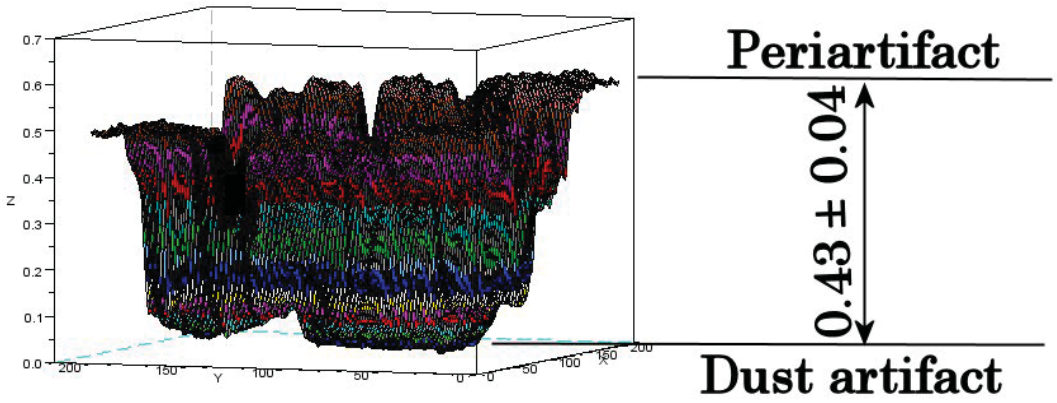

Fig. 10 V value for dust artifacts visualized in the artificial eye with a sunset-colored fundus

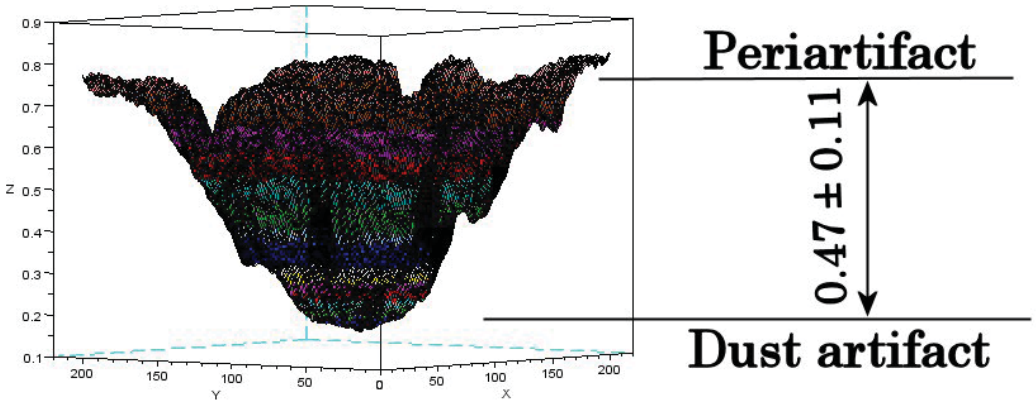

Fig. 11 V value for dust artifacts visualized in the artificial eye with a rose-colored fundus

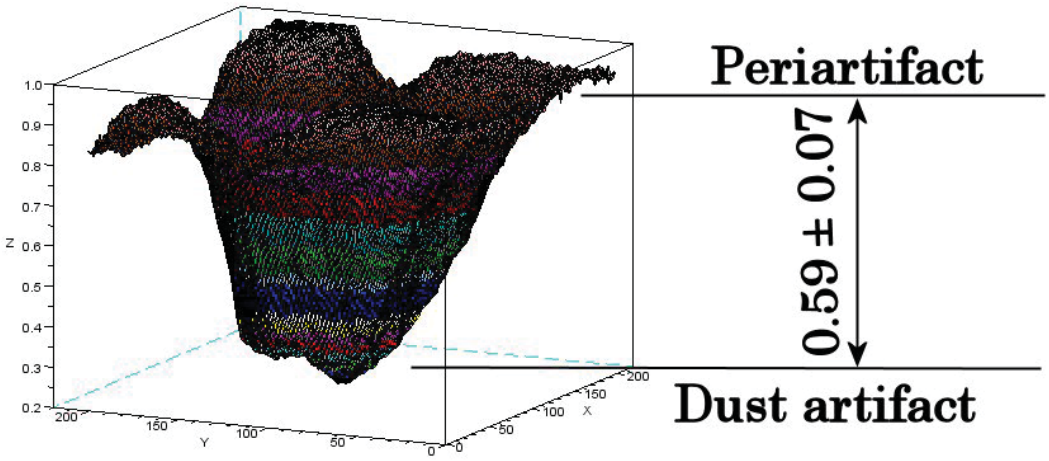

Fig. 12 V value for dust artifacts visualized in the artificial eye with a sunflower-colored fundus

D.Analysis of the HSV Color Space

Fig. 13 shows the average and standard deviations of the V values. In these graphs, the bars represent average values, whereas the lines represent standard deviations. The bars are colored to indicate hemorrhages, hard exudates, and photocoagulation marks. The artificial eye's fundi denote khaki, sunset, rose, and sunflower fundi, from the left to the right.

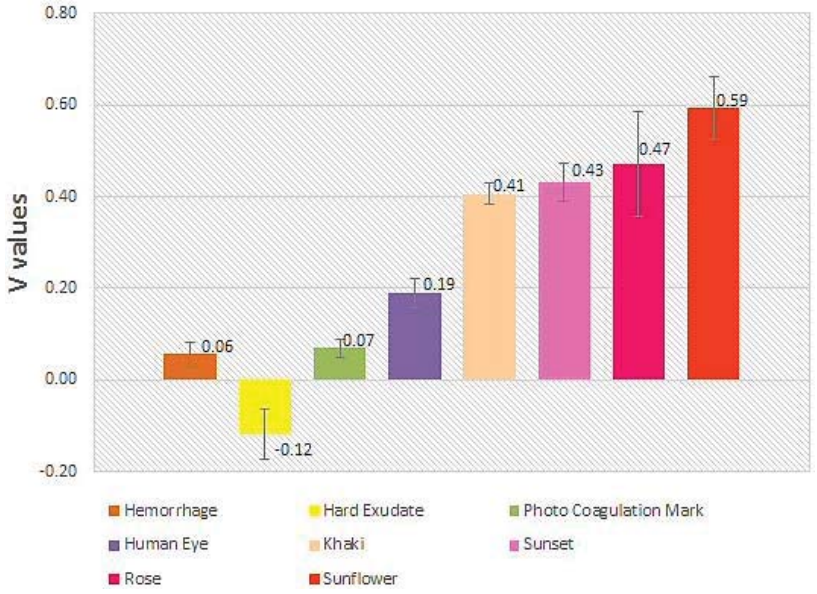

Fig. 13 The average and standard deviations of V values

E. Sensitivity Evaluation

Two ratios of dust artifacts to manifestation areas (sensitivity values) were determined for both the human and artificial eyes. The sensitivity values of the human eyes were 3.37 ± 0.56 (hemorrhages), −1.63 ± 0.27 (hard exudates), and 2.71 ± 0.45 (photocoagulation marks). Hemorrhages and photocoagulation marks were sensitive, as was the absolute value of the hard exudates. The sensitivity values of the artificial eyes were 8.44 ± 1.75, −4.08 ± 0.84, and 6.79 ± 1.41, for hemorrhages, hard exudates, photocoagulation marks, respectively. Hemorrhages and photocoagulation marks for the artificial eyes were more sensitive than those for the human eyes. The absolute value of the hard exudates for the artificial eyes was more sensitive than that for the human eyes. Furthermore, these absolute values were directly proportional to the sensitive capabilities of the V values.

IV. Discussion

The fundus color of a patient with diabetic retinopathy appears reddish brown. Therefore, this study used sunflower, rose, sunset, and khaki colors to replicate the fundus in an artificial eye. The V values of the HSV color space were successful in distinguishing small retinal hemorrhages, hard exudates, and photocoagulation marks from dust artifacts in patients with diabetic retinopathy. However, the hue and saturation values were not successful in distinguishing the same.

Acknowledgment

The photographs of patients with diabetic retinopathy were provided by Hiroshima University Hospital. The National Institute of Technology, Numazu College funded this research. We are very thankful to all those who helped in our study.

References

[1] T. Tsuchiya, "Measure Against Lifestyle Related Disease," JMAJ, Vol.49 No.3, 2006, pp.132-134.
[2] Z.T. Bloomgarden, "American Diabetes Association Annual Meeting, 1999, Diabetes and obesity," Diabetes Care, Vol.23, No.1, 2000, pp.118-124.
[3] S.S. Savant, H.B. Chandalia, "Diabetic retinopathy," Int J Diabetes Dev Ctries, Vol.10, 1999, pp.9-25.
[4] American Diabetes Association, "Diabetic retinopathy," Clinical Diabetes, Vol.19 No.1, 2001, pp.29-32.
[5] J.B. Brown, K.L. Pedula, K.H. Summers, "Diabetic retinopathy," Diabetes Care, Vol.26 No.9, 2003, pp.2637-2642.
[6] S. Garg, R.M. Davis, "Diabetic retinopathy screening update," Clinical diabetes 2009, Vol.27 No.4, 2009, pp.140-145.
[7] M.S. Figueroa, I. Contreras, S. Noval, "Anti-angiogetic drugs as an adjunctive therapy in the surgical treatment of diabetic retinopathy," Curr Diabetes Rev, Vol.5 No.1, 2009, pp.52-56.
[8] E. Fernández-Caldas, W.L. Trudeau, D.K. Ledford, "Environmental control of indoor biologic agents," J Allergy Clin Immunol, Vol.2 No.2, 1994, pp.404-412.
[9] A.G. Oomen, J.P.C.M. Janssen, A. Dusseldorp, et al., "Exposure to chemicals via house dust," RIVM Report 609021064, 2008, pp.11-18.
[10] M. Born, E. Wolf, "Principles of Optics 7th expanded edition, Electromagnetic Theory of Propagation, Interference and Diffraction of Light," Cambridge Univ Press, 1999.
[11] R.G. Willson, M.W. Maimone, A.E. Johnson, et al., "An Optical Model for Image Artifacts Produced by Dust Particles on Lenses," Proceedings of ISAIRAS 2005 Conference, 2005.
[12] A.V. Shukla, "Clinical Optics Primer for Ophthalmic Medical Personnel, A Guide to Laws, Formulae, Calculations, and Clinical Applications," SLACK Inc, 2009.
[13] D.D. David, R. Prescott, S. Kennedy, "Simultaneous stereoscopic fundus camera incorporating a single optical axis," Invest Ophthalmol Vis Sci March, 1980, pp.289-297.
[14] R. Zeimer, S. Zou, T. Meeder, et al., "A fundus camera dedicated to the screening of diabetic retinopathy in the primary-care physician's office," Invest Ophthalmol Vis Sci May, Vol. 43 No.5, 2002, pp.1581-1587.
[15] R.F. Lyon, "Prism-Based Color Separation for Professional Digital Photography," Proceedings of IS&T's PICS 2000 Conference: Image Processing, Image Quality, Image Capture Systems Conference, 2000, Oregon, USA, 2000.
[16] A.E. Dirik, H.T. Sencar, N. Memon, "Source Camera Identification Based on Sensor dust Characteristics," The proceedings of Signal Processing Applications for Public Security and Forensics 2007, SAFE'07, IEEE Workshop, 2007.

[17] A. Zamfir, A. Drimbarean, M. Zamfir, et al., "An Optic Model of the Appearance of Blemishes in Digital Photographs," Proceedings of SPIE 2007, Vol. 6502, Digital Photography 3, 2007.
[18] R. Bergman, R. Maurer, H. Nachlieli, et al., "Comprehensive Solutions for Removal of Dust and Scratches from Images," Journal of Electronic Imaging, Vol.17 No.1, 2008, pp.1-25.
[19] A.E. Dirik, H.T. Sencar, N. Memon, "Digital Single Lens Reflex Camera Identification From Traces of Sensor Dust," IEEE Trans Info For and Sec 2008, Vol.3 No.3, 2008, pp.539-552.
[20] N. Suzuki, "Basic Research for Distinguishing Small Retinal Hemorrhages from Dust Artifact by using Hue, Lightness, and Saturation Color Space," International Journal of Medical, Health, Biomedical, Bioengineering and Pharmaceutical Engineering, Vol.6, No.5, 2012, pp151-159.
[21] C.C. Thomas, "OPTICS", Springfield, 1968, pp.156-7.

Naoto Suzuki earned the necessary credits, but before receiving a Ph.D. degree, he left the doctoral course in Graduate School of Engineering, The University of Tokyo, in 2000. He performed research on an ophthalmologic device while working with a medical equipment maker and received a Ph.D. degree from Chiba University in 2007. He was an Assistant Professor at Hiroshima International University from 2009 to 2013. Since 2014, he has been an Associate Professor in National Institute of Technology, Numazu College.